

REFERENCES

1. R. L. McCrory, L. Montierth, R. L. Morse, and C. P. Verdon, *Laser Interaction and Related Phenomena* (Plenum, New York, 1981), Vol. 5, pp. 713-742.
2. B. A. Brinker, J. M. Cavese, J. R. Miller, S. G. Noyes, S. Sheble, and L. T. Whitaker, *J. Vac. Sci. Technol. A* **1**, 941 (1983).
3. S. L. Letts, D. W. Meyers, and L. A. Witt, *J. Vac. Sci. Technol.* **19**, 758 (1981).
4. M. C. Lee, I. Feng, D. D. Elleman, T. G. Wang, and A. T. Young, *J. Vac. Sci. Technol.* **20** (1982).
5. R. Liepins, M. Campbell, J. S. Clements, J. Hammond, and R. J. Fries, *J. Vac. Sci. Technol.* **18**, 1218 (1981).
6. Union Carbide, parylene technology brochure.
7. H. Kim, T. Powers, and J. Mason, *J. Vac. Sci. Technol.* **21**, 900 (1982).
8. D. Bancroft, *Phys. Rev.* **59**, 588 (1941).
9. W. E. Tefft, *J. Res. Nat. Bur. Stand. (U.S.) B* **64B**, 237 (1960).
10. R. Q. Gram, D. H. Douglass, and J. A. Tyson, *Rev. Sci. Instrum.* **44**, 857 (1973).
11. S. Gracewski (private communication).
12. LLE Review **9**, 21 (1981).

3.B Liquid Crystal Soft Apertures

High-quality, laser-beam apodization has been the goal of solid-state laser device research programs since the early 1970s. The ability to shape the spatial intensity profile of a low- to moderate-power laser beam, prior to propagation through several stages of amplification, to a large extent determines the ultimate performance of high-peak-power and high-average-power systems.

The effect of a perfect apodizer device is illustrated schematically in Fig. 24.21. With this element one can create a quasi-flat-topped intensity profile from a Gaussian input. The soft edges of the apodizer minimize the occurrence of Fresnel diffraction rings in the output beam, permitting its propagation and amplification with a large fill factor and minimal small-scale self-focusing.

A perfect apodizer preserves the temporal shape of the input pulse and causes little distortion to the phase across the transmitted beam profile. Transmission in the device clear aperture is close to 1.0, whereas transmission at the edge falls to less than 10^{-3} . Good circular symmetry of the apodizer is a requirement for most applications, as is an edge profile that approximates the transmittance function

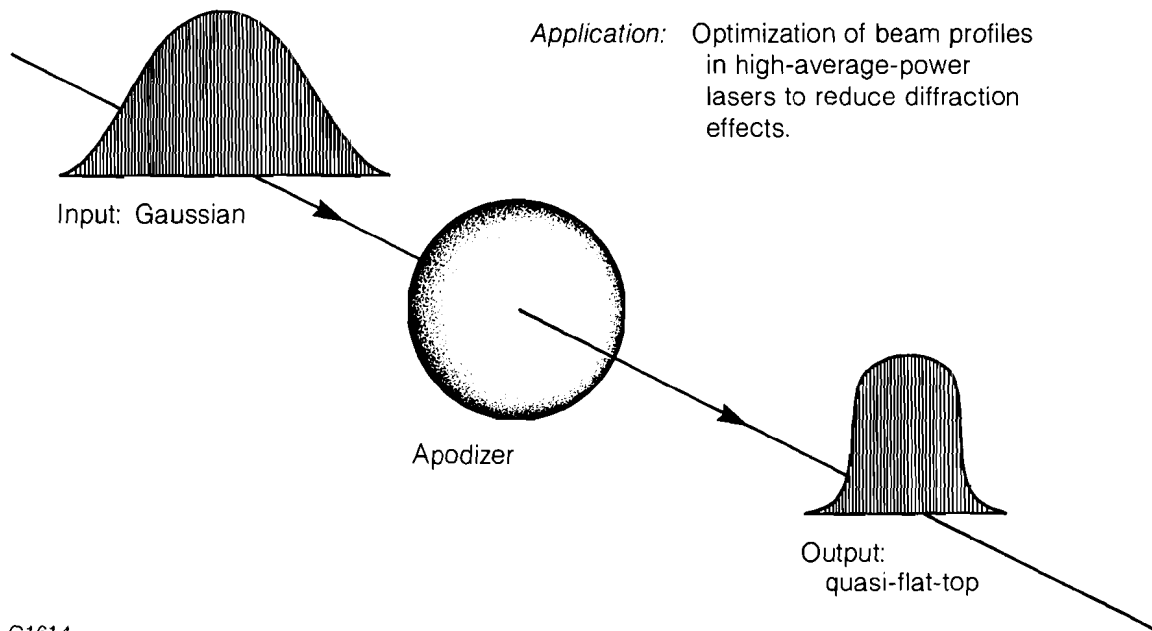


Fig. 24.21
Laser beam apodizer. A perfect apodizer truncates the wings of a Gaussian input without introducing diffraction effects. Good optical phase quality and intensity in the center of the beam are preserved.

$$I(r) = I_0 \exp[-(r/r_0)^N], \quad N = 5 \text{ to } 10, \quad (1)$$

where the radial clear aperture parameter r_0 is selected on the condition that $I(r_1) = 10^{-3} I_0$, where $2r_1$ is the entry aperture of the amplifying device that follows the apodizer.¹ Finally, the device must exhibit a high degree of laser damage resistance for high-peak-power applications, and low absorptive losses for high-average-power applications.

The fact that no perfect apodizer has been created is evident from the literature. The following passive-device technologies have been pursued:

- (1) shaped absorbing liquid cells²
- (2) saturable absorbers³
- (3) shaped solid absorbers^{2,4,5,6}
- (4) graded photographic emulsion^{2,7,8}
- (5) graded metallic films^{2,9}
- (6) single and multilayer dielectric films²
- (7) total internal reflection devices^{1,2,10}
- (8) radially birefringent elements¹²⁻¹⁵
- (9) annular lens¹⁶

Electro-optic and magneto-optic concepts have also been proposed,² but none of these passive or active approaches has found broad acceptance. In fact, most high-peak-power solid-state laser systems, like LLE's OMEGA, use a hard aperture and an image-relaying scheme

invented by Hunt *et al.*¹⁷ to maximize fill factor and minimize diffraction effects.

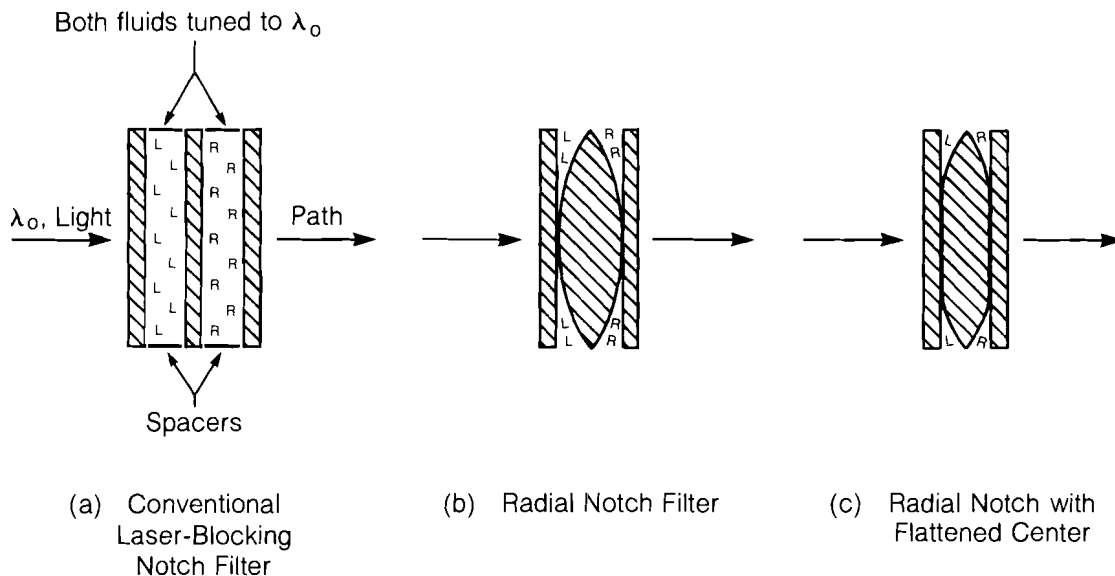
At LLE we have recently developed a new apodizer device based upon liquid crystal technology, which has demonstrated properties nearly like those of a perfect apodizer. Originating from our previous work with liquid crystal polarizers (LLE Review 21, 8) and laser-blocking notch filters (LLE Review 15, 30), our liquid crystal soft aperture possesses the following characteristics:

- (1) passive and nonabsorptive, with no aperture limitations
- (2) wavelength selectivity from UV to IR
- (3) no input polarization requirements
- (4) ease of fabrication in circular or other cross sections
- (5) high laser-damage resistance
- (6) low wave-front distortion

Fig. 24.22

Evolution of the concept for liquid crystal soft aperture. By changing the shape of the central spacer element in a conventional laser-blocking notch filter, we can synthesize filters with radially varying transmission profiles. Blocking extinction, which originates from the selective reflection effect, varies from zero at element center to greater than 10^3 at the edge. Refractive index matching between the fluids and the glass minimizes phase distortion.

The concept of a liquid crystal soft aperture follows directly from the operating principles of a laser-blocking notch filter. Figure 24.22 illustrates the evolution of the device. In the conventional liquid crystal notch filter of Fig. 24.22(a), the LH and RH fluids act as a pair of crossed circular polarizers for incident laser radiation at wavelength λ_0 . Light of any polarization state at that wavelength is reflected from the filter with a blocking efficiency approaching 10^4 , provided (1) that the thickness of each fluid layer is at least $11 \mu\text{m}$ and (2) that the internal pitch of each fluid is equal in magnitude but opposite in chirality. The



G1616

selective reflection effect can be made radially varying if curved surfaces are employed on the central spacer glass, as shown in Fig. 24.22(b). The fluid path is therefore made negligible at the center of the filter and increases to tens of micrometers at the filter edge. Blocking extinction increases radially with fluid layer thickness.

The cell geometry most useful for apodizer devices is illustrated in Fig. 24.22(c). Here, a biconvex central element has had optical flats polished onto the center of each curved surface. The flats determine the clear aperture of the apodizer, and the soft edge is created by the increase in LH and RH fluid layer thickness along the device radius. Fundamental to the success of the configuration shown in Fig. 24.22(c) is the ability to adjust the average refractive index of each liquid crystal layer to match that of the confining substrates to one part in 10^3 to 10^4 . This minimizes optical wave-front distortion across the device clear aperture and well into the soft edge. The reflective nature of the effect promotes a high laser-damage resistance and minimal thermally induced distortions at high average powers.

We have designed liquid crystal soft apertures for use at $\lambda = 1064 \text{ nm}$. The transmission profile of this type of apodizer at the soft edge is modeled by an equation of the form

$$I(r) = I_0 e^{-Qt(r)}, \quad (2)$$

where Q is a factor that describes the quality of liquid crystal alignment, and $t(r)$ is the LH or RH fluid gap thickness in micrometers. For flattened, spherical central spacer elements, the functional form for t is given as

$$t(r, \text{ microns}) = \frac{r^2 - r_0^2}{4f(n - 1)} \times 10^3 \quad (r \geq r_0), \quad (3)$$

where $r_0 =$ radius of flattened clear aperture [as defined in Eq. (1)]
in mm,

$r =$ radial distance from the center of the device, in mm,

$f =$ focal length of biconvex lens, in mm, and

$n =$ refractive index of lens material, at λ_0 .

Measurements on numerous notch filter cells have shown that Q varies depending upon the method and materials we choose to use in the preparation of our substrates. Figure 24.23 specifies those substrate surfaces that require a unidirectional rub with $1/10\text{-}\mu\text{m}$ diamond paste. (As previously described,^{14,18} macroscopic alignment of liquid crystal molecules must be externally induced by the creation of microgrooves.) Because we have only recently begun to work with curved surfaces, we have experienced some variability in alignment results on the central spacer element of our soft apertures. Figure 24.24 shows the degree of blocking extinction as a function of fluid gap thickness for a *well-aligned*, wedged notch filter. Equation (2) fits the experimental data with a Q factor of 0.34.

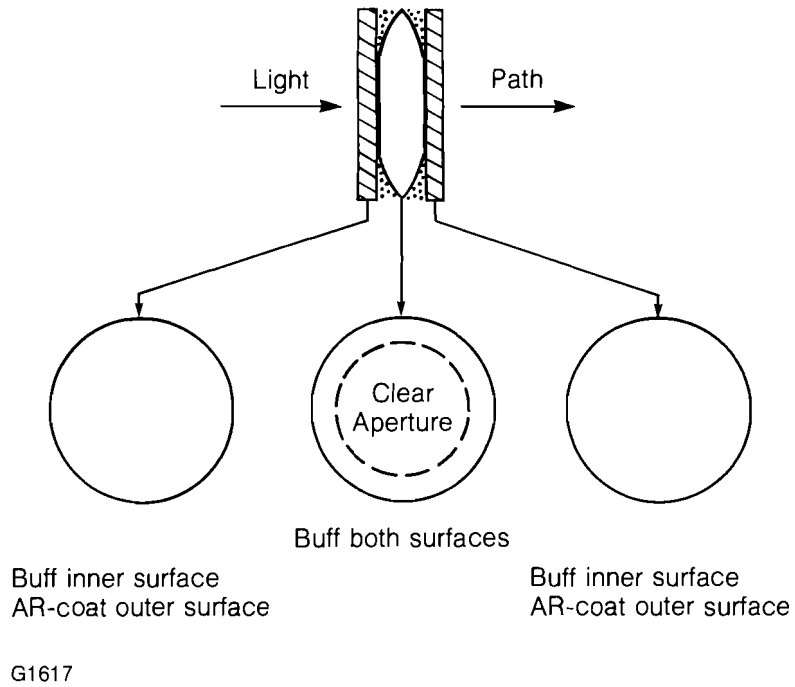


Fig. 24.23
Liquid crystal soft aperture construction. Unidirectional rubbing of substrate inner surfaces is required prior to cell assembly. This promotes macroscopic alignment of the liquid crystal molecules over apertures of several cm.

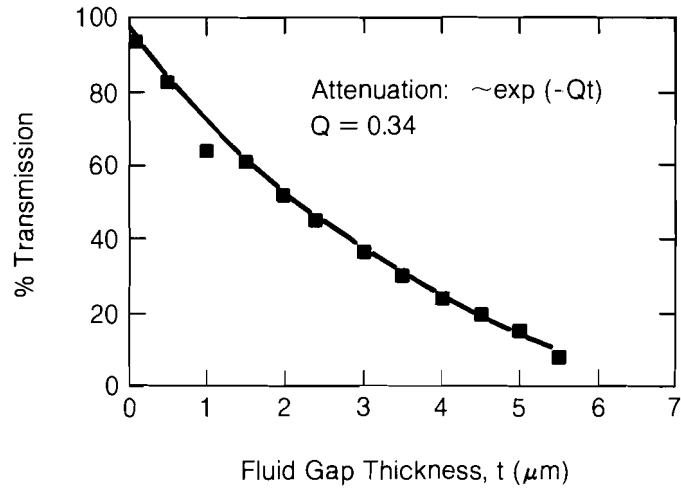


Fig. 24.24
Notch filter transmittance as a function of fluid gap thickness at $\lambda = 1064 \text{ nm}$. This data is required to estimate the thickness dependence of the blocking extinction in the edge region of the liquid crystal soft aperture.

*Data not corrected for Fresnel reflection losses

G1618

We have fabricated and constructed several prototype soft apertures, based on the design considerations described above. The dimensions and transmission profile of a 1064-nm soft aperture are given in Fig. 24.25. The profile was generated by scanning across the apodizer with a linearly polarized Nd:YAG laser beam whose focused beam waist was $150 \mu\text{m} \pm 10\%$ in dimension ($1/e^2$). (The noise in the profile is due to instabilities in the scanning laser and is not a result of any defects in the apodizer.) Interferometry at 1064 nm, also performed on this soft aperture, was used to determine the amount of wave-front distortion in the area of the soft edge. The transmission profile is replotted in Fig. 24.26 against the wave-front distortion. Figure 24.26 demonstrates that, with index matching to one part in 10^3 and temperature control to $\pm 2^\circ\text{C}$ (the temperature coefficient of the refractive index for our fluids is approximately $-3 \times 10^{-4}/^\circ\text{C}$), we can keep wave-front distortion below 0.25 waves at a point on the soft edge where transmittance drops to 20%. Glass apodizers exhibit a wave-front distortion in excess of 1.2 waves at their 20% transmittance point.

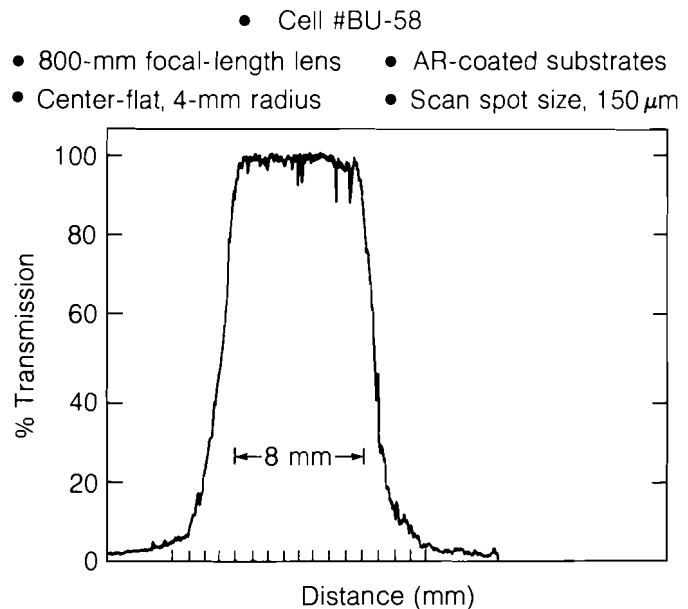
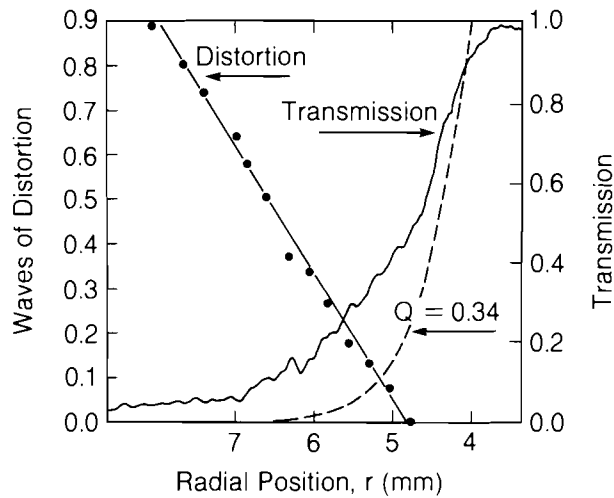


Fig. 24.25
Transmission profile scan for a liquid crystal soft aperture at $\lambda = 1064 \text{ nm}$.

The calculated transmittance profile, using Eqs. (2) and (3) and the appropriate constants ($f = 800 \text{ mm}$, $r_0 = 4 \text{ mm}$, $n = 1.50$), fits the measured one in Fig. 24.26 if a Q factor of 0.17 is assumed. This suggests that the quality of alignment is adequate, but not optimal. Improved alignment would steepen the profile to that depicted by the dotted line in Fig. 24.26. This would further improve the wave-front quality of the device.

Liquid crystal soft apertures have been made and delivered to experimentalists outside of LLE for testing and evaluation. The high laser

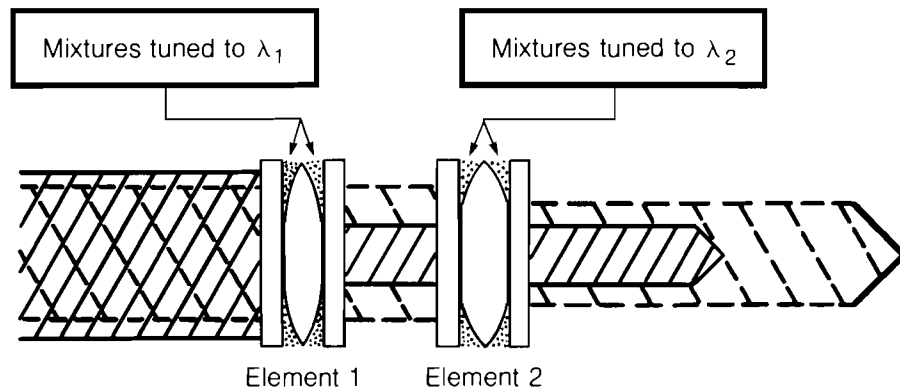
- Scan spot size: 150 μm
- Cell #BU-58, 800-mm focal length
- Center-flat, 4-mm radius
- Measurement wavelength: 1064 nm



G1621

Fig. 24.26

Phase distortion in the edge region of a liquid crystal soft aperture. An enlargement of the transmission scan from Fig. 24.25 is superimposed upon phase distortion measurements made with interferometry at 1064 nm. Wave-front distortion less than $\lambda/4$ is maintained out to the point where transmission drops to 20%. Improvements in the quality of liquid crystal alignment (see dashed curve) will reduce wave-front distortion to less than $\lambda/10$.



G1622

Fig. 24.27

Liquid crystal soft aperture flexibility. Because the selective reflection effect in liquid crystals is wavelength specific, liquid crystal soft apertures may be stacked in tandem to operate on collinearly propagating laser beams whose wavelengths differ. Light at a given laser wavelength may be apodized with a unique clear aperture size and soft edge profile without affecting light at other wavelengths. No other technology exists that can perform in a similar fashion.

damage resistance¹⁸ and low absorption of the liquid crystal compounds used to construct this device should permit its use in high-peak and high-average-power systems operating in the UV to near IR. The wavelength selectivity of the selective reflection effect permits apodization of one wavelength only, in situations where two or more wavelengths propagate collinearly (see Fig. 24.27). No other technology exists that can perform in a similar fashion.

ACKNOWLEDGMENT

This work was supported by contracts with the Advanced Laser Technology Group at General Electric Company, Binghamton, NY.

REFERENCES

1. I. K. Krasnyuk *et al.*, *Sov. J. Quantum Electron.* **6**, 725 (1976).
2. V. R. Costich and B. C. Johnson, *Laser Focus*, 43, (September 1974).
3. A. Penzkofer and W. Frölich, *Opt. Commun.* **28**, 197 (1979).
4. Y. Asahara and T. Izumitani, U.S. Patent No. 4108621 (22 August 1978).
5. G. Dubé, *Advanced Laser Technology and Applications* (SPIE, Bellingham, WA, 1982), Vol. 335, p.10.
6. V. I. Kryzhanovskii, *Sov. J. Quantum Electron.* **13**, 194 (1983).
7. A. J. Campillo, B. Carpenter, B. E. Newnam, and S. L. Shapiro, *Opt. Commun.* **10**, 313 (1974).
8. E. W. S. Hee, *Optics and Laser Technology*, 75 (April 1975).
9. S. B. Arifzhanov *et al.*, *Sov. J. Quantum Electron.* **11**, 745 (1981).
10. G. Dubé, *Opt. Commun.* **12**, 344 (1974).
11. J. C. Diels, *Appl. Opt.* **14**, 2810 (1975).
12. S. B. Papernyi, V. A. Serebryakov, and V. E. Yashin, *Sov. J. Quantum Electron.* **8**, 1165 (1978).
13. G. Giuliani, Y. K. Park, and R. L. Byer, *Opt. Lett.* **5**, 491 (1980).
14. S. D. Jacobs, *Polarizers and Applications* (SPIE, Bellingham, WA, 1981), Vol. 307, p.98.
15. J. M. Eggleston, G. Giuliani, and R. L. Byer, *J. Opt. Soc. Am.* **71**, 1264 (1981).
16. B. J. Feldman and S. J. Gitomer, *Appl. Opt.* **16**, 1484 (1977).
17. J. T. Hunt, J. A. Glaze, W. W. Simmons, and P. A. Renard, *Appl. Opt.* **17**, 2053 (1978).
18. S. D. Jacobs, K. A. Cerqua, T. J. Kessler, W. Seka, and R. Bahr, LLE Report No. 163, to be published as *NBS Special Publication: 16th Annual Symposium on Optical Materials for High-Power Lasers, Boulder, CO, October 1984*.